Two-Dimensional Peripheral Refraction and Image Quality for Four Types of Refractive Surgeries

Zhenghua Lin, MS; Yiqiu Lu, MS; Pablo Artal, PhD; Zhikuan Yang, MD, PhD; Weizhong Lan, MD, PhD

ABSTRACT

PURPOSE: To provide a comprehensive investigation of the optical quality across the visual field for current mainstream types of refractive surgeries.

METHODS: Sixty eyes from 60 adults who received refractive surgery of either femtosecond laser–assisted laser in situ keratomileusis (FS-LASIK), Q-value guided customized laser in situ keratomileusis (Q-LASIK), small incision lenticule extraction (SMILE), or Implantable Collamer Lens (ICL) (STAAR Surgical) implantation were included in this study. Refraction and optical aberrations from a visual field of horizontal 60° (from temporal 30° to nasal 30°) and vertical 36° (from superior 20° to inferior 16°) were measured using a custom-made Hartmann-Shack wavefront peripheral sensor. Refractive error, higher order aberrations, point spread function (PSF), and Strehl ratio were compared among these groups prior to and after the surgical procedures, respectively.

RESULTS: All types of surgical procedures achieved an almost plano refraction in the central retina. This was also the case in the peripheral retina for the three types of laser refractive surgeries. However, residual peripheral relative hyperopic defocus was observed after ICL implantation. In all groups prior to the surgery, PSFs showed increasing distortion with eccentricity and arrow-like shape pointing toward the central fovea in the periphery in diagonals. Degradation of the PSFs was diminished by all three types of laser refractive surgeries, whereas ICL implantation made the peripheral distortion more prominent.

CONCLUSIONS: Although ICL implantation produced a similar impact on refractive correction and objective optical quality in the central vision compared with other laser refractive surgeries, its outcome on the peripheral optics is different. The impact of this difference on visual performance deserves notice and warrants further investigation.

[*J Refract Surg*. 2023;39(1):40-47.]

Refractive surgery has gained increasing popularity in young adults with myopia,[1] because it could have a rapid acquisition of postoperative sharp vision and significantly improve sports experience.[2] The main options of refractive surgery currently include laser refractive surgery and Implantable Collamer Lens (ICL) (STAAR Surgical) implantation, both of which are able to bring good postoperative visual quality to patients.[3,4]

However, the existing research mostly focuses on the optical quality of foveal vision, whereas investigation of

From Aier School of Ophthalmology, Central South University, Changsha, China (ZL, YL, PA, ZY, WL); Aier School of Optometry, Hubei University of Science and Technology, Xianning, China (ZY, WL); Guangzhou Aier Eye Hospital, Jinan University, Guangzhou, China (WL); Laboratorio de Óptica, Universidad de Murcia, Campus de Espinardo, Murcia, Spain (ZL, PA); Hunan Province International Cooperation Base for Optometry Science and Technology, Changsha, China (ZL, YL, PA, ZY, WL); and Hunan Province Optometry Engineering and Technology Research Center, Changsha, China (ZL, YL, PA, ZY, WL).

Submitted: May 26, 2022; Accepted: November 15, 2022

Supported by Key Research and Development Project of Science & Technology Department of Hunan Province (Grant No. 2019SK2051), Key Research and Development Project, Ministry of Science & Technology, China (Grant No. 2022YFE0124600), Science and Technology Service Network Initiative, Chinese Academy of Sciences (Grant No. KFJ-STS-QYZD-2021-11-001), and an intramural grant by Aier Eye Hospital Group (Grant No. AR1903D2).

Disclosure: The authors have no financial or proprietary interest in the materials presented herein.

Drs. Lin and Lu contributed equally to this work and should be considered as equal first authors.

Correspondence: Weizhong Lan, MD, PhD (lanweizhong@aierchina.com) and Zhikuan Yang, MD, PhD (yangzhikuan@aierchina.com), Aier School of Ophthalmology, Central South University, Changsha, 410000, China.

doi:10.3928/1081597X-20221115-01

the peripheral field is rather rare. The optical quality in the peripheral visual field also has great impact on living quality, especially in detecting motion and orientation.[5,6] The major complaints about visual symptoms after surgery include glare, ghosting, and halos.[7] The distortion of the retinal image can be interpreted by lower order or higher order aberrations (HOAs), but from previous studies, it seems that the visual complaints are more relevant with some HOAs, such as coma and spherical aberration.[8]

In the current study, we used a custom-made Hartmann-Shack wavefront peripheral autorefractor (Voptica Peripheral Refraction; Voptica SL)[9-11] to evaluate the image quality in both the central fovea and peripheral retina, with the measured field corresponding to horizontally within 60° (from temporal 30° to nasal 30°) and vertically within 36° (from superior 20° to inferior 16°). Based on the findings, we aimed to investigate the aberrations across the visual field and to provide more comprehensive understanding of optical quality for these popular refractive surgeries.

PATIENTS AND METHODS

This was a prospective study performed at Changsha Aier Eye Hospital from February 2020 to June 2020. All participants were informed about the content of the study and signed a consent form prior to commencement. All procedures followed the tenets of the Declaration of Helsinki and the study was approved by the Institutional Review Board of AIER Eye Hospital Groups (AIER-2020IRB02). The participants in this study needed to finish on- and off-axis refraction examinations prior to and 3 months after the refractive surgery to explore whether different surgical procedures will cause changes in peripheral refraction and further affect the visual quality.

PATIENTS

Patients who sought refractive surgery and met the study criteria were invited to participate. The inclusion criteria were: age older than 18 years, myopia degree not smaller than -5.00 diopters (D); astigmatism of no greater than 2.00 D, corrected distance visual acuity (CDVA) of 20/20 or better, and stable refraction for 2 years. Patients with systematic diseases, a history of ocular surgery or trauma, or a history of ocular disorder other than myopia or astigmatism were excluded.

SURGERY OPTIONS

ICL Implantation. The ICL is a plate-haptic single-piece intraocular lens made of Collamer, which is a flexible, hydrophilic material consisting of HEMA hydrogel, water, and porcine collagen. It can be folded and implanted in the posterior chamber via a 2.8- to 3.2-mm corneal incision. It has a high degree of biocompatibility, good permeability of gases and metabolites, and good absorption of ultraviolet radiation.[12] The ICL model used in this study was the ICL V4c, which was a 6-mm wide lens and came in four sizes (12.1, 12.6, 13.2, and 13.7 mm in depth—the specific size depends on the anterior chamber depth and the horizontal white-to-white diameter). Its optic zone diameter was 4.9 to 5.8 mm, with a spherical power range of -0.50 to -18.00 D and a cylindrical power range of +0.50 to +6.00 D. All ICL surgical procedures were performed by the same surgeon.

Laser Refractive Surgery. The laser refractive surgery in this study included small incision lenticule extraction (SMILE), femtosecond laser–assisted laser in situ keratomileusis (FS-LASIK), and Q-value guided customized laser in situ keratomileusis (Q-LASIK). In the SMILE procedures, a 500-kHz VisuMax femtosecond laser system (Carl Zeiss Meditec AG) was used. The lenticule diameter was set between 6 and 6.5 mm; the cap diameter was set to (7.6 mm for 10 patients, 7.3 mm for 6 patients; average = 7.42 mm) at a 120-µm depth, according to individual condition. A 90° single-side cut, with a length of 2 mm, was created during the procedure. In the FS-LASIK and Q-LASIK procedures, the WaveLight FS-200 femtosecond laser (Alcon Laboratories, Inc) was used for flap creation. Flap diameters were 8.5 to 9 mm and the thickness was 110 µm. The planned optic zone was set between 6 and 6.5 mm. All FS-LASIK and Q-LASIK surgical procedures were performed by the same surgeon.

MEASURE OF ON- AND OFF-AXIS REFRACTION

The on- and off-axis refraction in the right eye was measured with a customized open-view Hartmann-Shack wavefront sensor (Voptica Peripheral Refraction).[9-11] An optical arm with the Hartmann-Shack sensor is mounted on a motor that can scan horizontally within 60° visual field (in 1° steps) in 1.3 seconds while the participants look at a distant target. The instrument is equipped with appropriate software to cope with large defocus values with a range of more than 10.00 D. A total of 10 targets were placed vertically in front of the participant, with the same angular distance between each pair of neighboring targets (corresponding to the visual field from superior 20° to inferior 16°). The centration of participants during the measurements was achieved by one real-time pupil camera and one real-time Hartmann-Shack camera to monitor the movement of the eye. If the patient does not follow the instruction, this could be easily recognized by the operator and corrected. This ensured that the data were collected accurately for each patient and condition. Thus, the two-dimensional retinal refraction map was retrieved from 10 horizontal scans

TABLE 1

Demographics of Patients Before and After Refractive Surgery for 3 Months[a]

Parameter	FS-LASIK (n = 11)	Q-LASIK (n = 21)	SMILE (n = 15)	ICL (n = 13)	P^b
Male/female (%)	27.3/72.7	33.3/66.7	26.7/73.3	23.1/76.9	
Age (year)	23.9 ± 6	22 ± 3.6	22.9 ± 4.3	22.8 ± 5.4	
SER (D)					
Preoperative	-7.60 ± 1.40	-7.80 ± 1.10	-7.20 ± 1.10	-8.80 ± 1.20	.007 (ICL vs SMILE)
Postoperative	-0.50 ± 0.20	-0.70 ± 0.30	-0.70 ± 0.30	-0.50 ± 0.40	.124
Change	7.00 ± 1.40	7.10 ± 1.10	6.50 ± 1.00	8.40 ± 1.20	
P^c	< .001	< .001	< .001	< .001	
Pupil diameter (mm)					
Preoperative	3.3 ± 0.7	4.1 ± 1.7	3 ± 0.6	3.2 ± 0.6	.123
Postoperative	3.1 ± 0.8	3.6 ± 1	2.9 ± 0.4	3.4 ± 0.6	.015 (Q-LASIK vs SMILE)
Change	-0.1 ± 0.6	-0.5 ± 1.3	-0.1 ± 0.3	0.2 ± 0.9	
P^c	.484	.11	.236	.44	
Corneal power (D)					
Preoperative	42.5 ± 0.8	42.4 ± 1.2	42.3 ± 1.4	42.4 ± 0.8	.812
Postoperative	36.9 ± 1	-36.9 ± 2.2	37 ± 1.3	42.7 ± 0.9	< .001 (FS-LASIK vs ICL; Q-LASIK vs ICL; SIMLE vs ICL)
Change	-5.58 ± 1	-5.5 ± 1.7	-5.24 ± 0.9	0.3 ± 1	
P^c	< .001	< .001	< .001	.278	

D = diopters; FS-LASIK = femtosecond laser–assisted laser in situ keratomileusis; ICL = Implantable Collamer Lens (STAAR Surgical) implantation; Q-LASIK = Q-value guided customized laser in situ keratomileusis; SER = spherical equivalent refraction; SMILE = small incision lenticule extraction

[a]Values are presented as mean ± standard deviation.

[b]P value for comparison among refractive surgery groups tested using the Kruskal-Wallis test. A GROUP vs GROUP term was used to show significant difference in pairwise comparison following the Kruskal-Wallis test.

[c]P value for comparison between preoperatively and postoperatively tested using the paired t *test.*

(resolution = 61 × 10). To maintain consistency between horizontal and vertical resolution of the map, a spline-based interpolation was applied and produced the final map (resolution = 61 × 37, 2,257 pixels). The measurement was performed in a room with dim light. After the measurement, spherical equivalent refraction (SER) was estimated in a 3-mm circular region of the center of the Hartmann-Shack image, whereas Zernike coefficients were determined in a 4-mm circular pupil diameter. The detailed procedure for generating the two-dimensional map[9-11] and more information about the instrument has been published elsewhere.[13,14]

Data Processing and Presentation

Data processing and graphics production were done using Matlab software (Math Works, Inc). The relative peripheral refractive maps were obtained by subtracting the data of the central retina from those of individual points of the map. The x-axis was always pointing right and the y-axis was always pointing upward in the coordinates, wherein a negative value represents temporal ocular or inferior ocular and a positive value represents nasal ocular or superior ocular. To better demonstrate the value in the peripheral field, two-dimensional maps were uniformly divided into multiple regions by eight horizontal lines with an interval equal to 4° and 11 vertical lines with an interval equal to 5°. The mean refractive value of the region was shown in the corresponding box of the map. The root mean square (RMS) of HOAs was calculated from Z6 to Z20. The Strehl ratio and the point spread functions (PSFs) were calculated from the measured aberrations. Each PSF image corresponded to 1 point of the peripheral field (the schematic is presented in **Figure A**, available in the online version of this article).

Statistical Analyses

Descriptive data are presented as mean ± standard deviation or median (quartile 25%, quartile 75%) [minimum value, maximum value]. The paired *t* test for normally distributed data or the Kruskal-Wallis test for not normally distributed data was used to compare the difference between preoperatively and postoperatively. The differences among the four refractive surgeries were examined using Matlab software by a

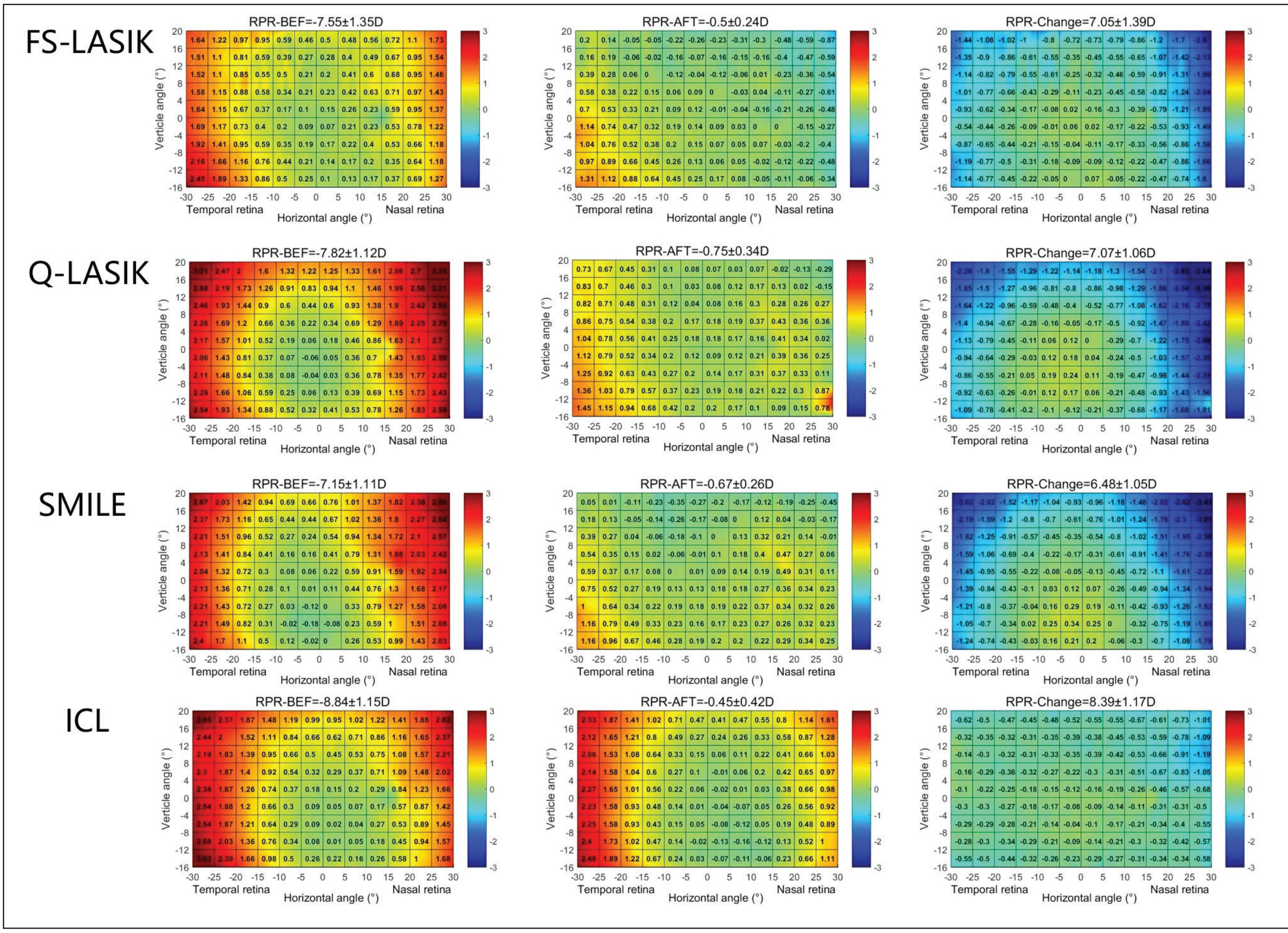

Figure 1. Average relative peripheral refraction map. The color code is in diopters. Left column: preoperative map. Middle column: postoperative map. Right column: difference map (postoperative minus preoperative). The mean value in the local region is showing the center of the corresponding box (size: 5° × 4°). The two-dimensional retinal relative peripheral refraction was generated from subtracting central refraction of two-dimensional peripheral refraction map. Each row corresponding to one type of surgery. FS-LASIK = femtosecond laser–assisted laser in situ keratomileusis; ICL = Implantable Collamer Lens (STAAR Surgical) implantation; Q-LASIK = Q-value guided customized laser in situ keratomileusis; SMILE = small incision lenticule extraction

one-way analysis of variance test. Pairwise comparison following the Kruskal-Wallis test was evaluated by SPSS software (SPSS, Inc). A two-tailed *P* value less than .05 was considered statistically significant.

RESULTS

The study comprised 60 right eyes from 60 adults, with a mean age of 22.7 ± 4.6 years (range: 18 to 35 years). The mean SER of all patients prior to surgery was -7.80 ± 1.30 D (range: -10.60 to -4.50 D) and then decreased to -0.60 ± 0.30 D (range: +0.40 to -1.30 D) after surgery. At baseline, no statistical difference was found in the total power of the corneal vertex and pupil diameter among the groups, but the degree of myopia was significantly higher in the ICL group (ICL vs SMILE, -8.20 ± 1.20 vs -7.20 ± 1.10 D, adjusted $P = .003$). After surgery, no statistical difference was found in SER among the groups. As expected, a significant reduction in the vertex power was found in the FS-LASIK, Q-LASIK, and SMILE groups after surgery, resulting in a significantly smaller power compared to the ICL group (**Table 1**). The averaged corneal power maps are shown in **Figure B** (available in the online version of this article).

Two-Dimensional Peripheral Refraction and HOA Maps

Figure 1 shows the retinal relative peripheral refraction map. Before the surgery, all groups presented relative hyperopia in the peripheral retina, which is especially prominent (ie, > 1.00 D) outside the eccentricity of 20° visual field. After the surgery, however, the relative refraction in the periphery reduced significantly in the laser refractive surgery groups, resulting in a relatively flat retinal refraction. In contrast, the ICL group maintained the relative hyperopia in the pe-

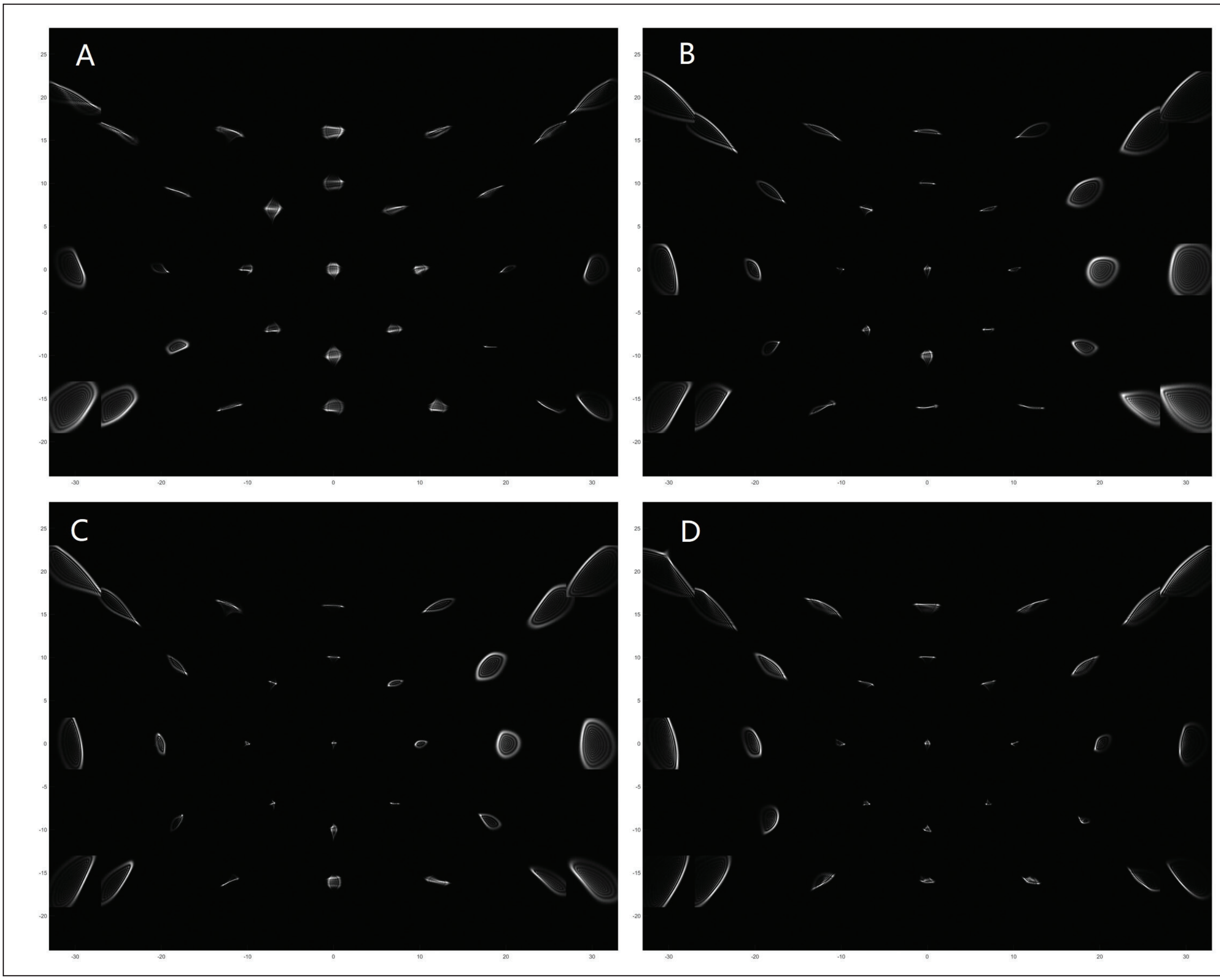

Figure 2. The point spread function (PSF) images prior to surgery: (A) femtosecond laser–assisted laser in situ keratomileusis (FS-LASIK), (B) Q-value guided customized laser in situ keratomileusis (Q-LASIK), (C) small incision lenticule extraction (SMILE), and (D) Implantable Collamer Lens (STAAR Surgical) implantation. The simulated angle of the PSF image is within 60 × 60 arc minutes.

riphery after surgery. From the difference maps (postoperatively minus preoperatively), it was shown that laser surgery (FS-LASIK, Q-LASIK, and SMILE) had a weaker modification in the peripheral than the central field (approximately 1.00 to 1.50 D difference, eccentricity 25° to 30°) compared with ICL implantation.

The aberrations in the foveal retina were expressed using Zernike coefficients. The RMS of corresponding higher order and total HOAs were also calculated. Prior to surgery, the difference among the groups were significant in Z4 (defocus, $P = .006$, Kruskal-Wallis test; SMILE vs ICL, adjusted $P = .003$), Z6 (oblique trefoil, $P = .039$, Kruskal-Wallis test; FS-LASIK vs Q-LASIK, adjusted $P = .025$), and RMS HOAs (higher order RMS, $P = .014$, Kruskal-Wallis test; FS-LASIK vs Q-LASIK, adjusted $P = .018$). After surgery, the difference among the groups was significant in Z5 (with-the-rule/against-the-rule astigmatism, $P = .001$, Kruskal-Wallis test; ICL vs FS-LASIK, adjusted $P = .002$, ICL vs Q-LASK, adjusted $P = .002$, ICL vs SMILE, adjusted $P = .038$), Z6 ($P = .025$, Kruskal-Wallis test), Z7 (vertical coma, $P = .01$, Kruskal-Wallis test; SMILE vs ICL, adjusted $P = .014$), Z9 (horizontal trefoil, $P = .005$, Kruskal-Wallis test; Q-LASIK vs SMILE, adjusted $P = .002$), and Z12 (spherical aberration, $P = .016$, Kruskal-Wallis test; FS-LASIK vs SMILE, adjusted $P = .011$). The comparison between preoperative and postoperative aberrations were tested by the paired *t* test. For the FS-LASIK group, the significant changed coefficients include Z4, Z5, and Z9. For the Q-LASIK group, the significant changed coef-

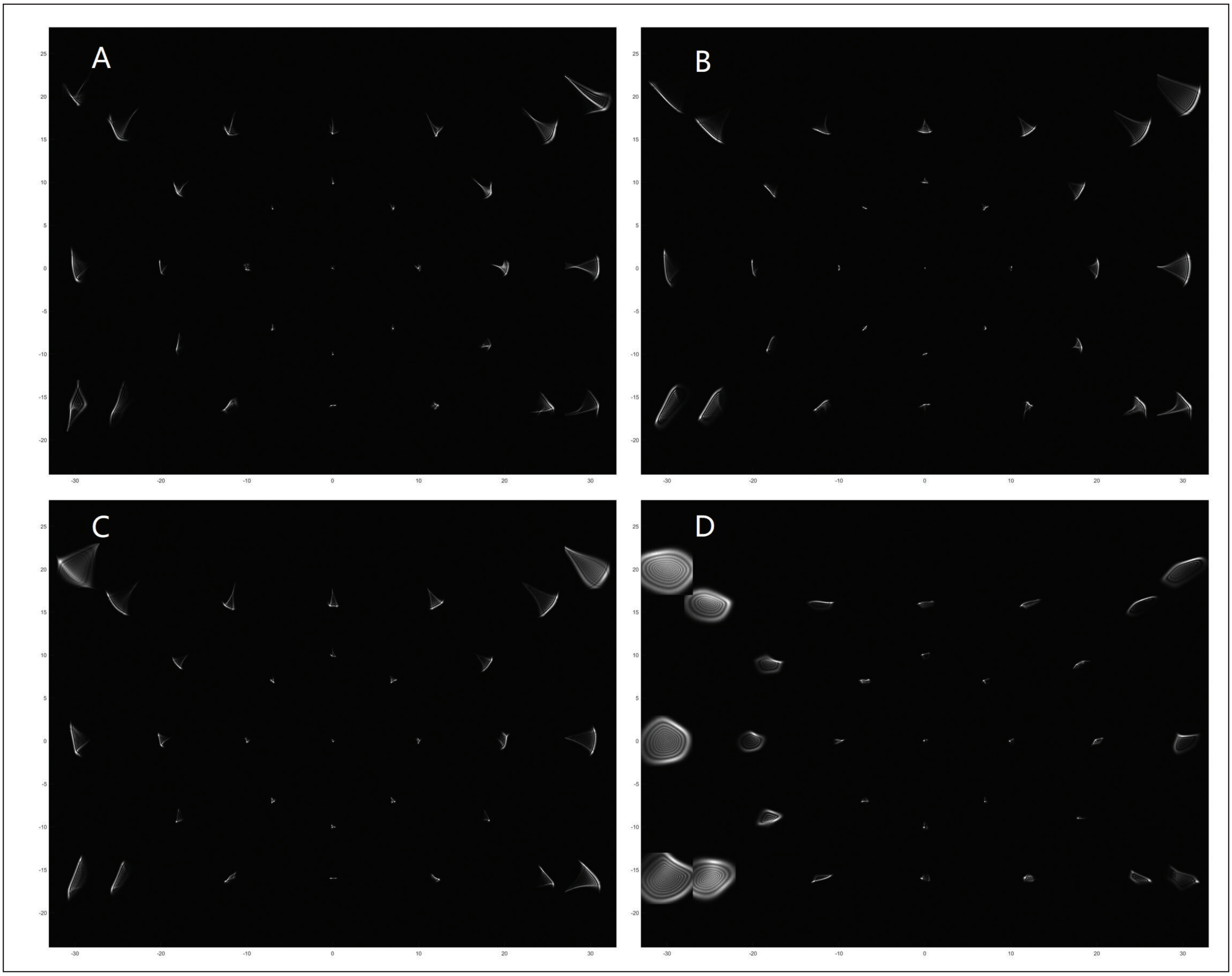

Figure 3. The point spread function (PSF) images after surgery: (A) femtosecond laser–assisted laser in situ keratomileusis (FS-LASIK), (B) Q-value guided customized laser in situ keratomileusis (Q-LASIK), (C) small incision lenticule extraction (SMILE), and (D) Implantable Collamer Lens (STAAR Surgical) implantation. The simulated angle of the PSF image is within 60 × 60 arc minutes.

ficients include Z4, Z5, and RMS HOAs. For the SMILE group, the significant changed coefficients include Z4, Z5, Z7, and Z9. For the value of RMS, only the Q-LASIK group showed a significant decrease in third-order RMS and RMS HOAs. More details are shown in **Tables A-D** (available in the online version of this article).

Retinal Image Quality and PSF

The peripheral PSF images show that the shells have an obvious direction, such as an arrow pointed toward the central fovea in the periphery in diagonals in all groups prior to the surgery (**Figure 2**). In the central vertical meridian, the direction of the long axis of the shell is parallel to the horizontal axis. The Q-LASIK and SMILE groups have a more prominent defocus image in the peripheral 20° to 30°, which are coincident with the peripheral refraction map in **Figure 1**. However, after laser surgery, the peripheral PSF image of the FS-LASIK, Q-LASIK, and SMILE groups changed the direction for almost 90° (**Figure 3**) (**Figures C-J**, available in the online version of this article). The component of defocus was also minimized in all groups, except for the ICL group in the temporal retina.

Retinal Image Quality

Strehl ratio is a common parameter to evaluate image quality in optical systems, which also can be considered as the area under the curve of the modulation transfer function. We analyzed the Strehl ratio for the peripheral and central retina, but no statistical difference could be found in any region. More details are presented in **Figure K** (available in the online version of this article) and **Table E** (available in the online version of this article).

DISCUSSION

To the best of our knowledge, this is the first study on refraction and other objective image quality across the retina with high resolution after different types of refractive surgery. Our results show that all types of procedures successfully corrected the central refractive error, but they had different impacts on the peripheral refraction and aberrations. Overall, the laser refractive surgery procedures produced a nearly flat refraction across the measured field. On the other hand, ICL implantation did not exert significant changes in the peripheral refraction, leading to an almost identical retinal refraction pattern before and after surgery. Again, ICL implantation was found to produce more prominent PSF distortion in the periphery compared with other surgical procedures.

With the progression of myopia, there is a greater relative peripheral hyperopia with the increase of central myopia. Because the femtosecond laser decreases the rate of stromal ablation from the central to peripheral cornea,[15,16] femtosecond-laser–based techniques, such as FS-LASIK and SMILE, induce a decreased correction of corneal refractive power with the eccentricity. Our results confirmed that this refractive correction pattern in the cornea led to an outcome of "emmetropia" pattern across the measured field of the retina. Thanks to the guidance of the corneal topographer, Q-LASIK also achieved a similar correction effect. In contrast, ICL implantation, given its even refractive power across the eccentricity, exerted an identical correction effect across the retina and maintained relative hyperopia in the periphery compared with prior to the surgery. It is unknown which postoperative pattern offers more benefit to the patients, because central vision dominates in most scenarios in the real world.[17-20] However, under some specific circumstances that also need good peripheral vision, such as in detecting motion and orientation[5,6] in driving or playing sports,[21-23] an outcome of the emmetropia pattern in a wider visual field might augment the visual performance. Some scholars have noticed this and imbedded this concept into an artificial intraocular lens by controlling the field curvature and reducing the astigmatism in the peripheral retina.[24,25]

In diagonals in the visual field, it was observed that the shape of the PSF was similar to a flat shell, with the long axis indicating 135° or 45°. This seems to be a compromise of intraocular astigmatism with central retina as the valley bottom of a prolonged eyeball. In the central vertical meridian, the long axis of the shell-shape distortion is almost parallel to the ground. This might be a major contribution from corneal astigmatism (with-the-rule astigmatism).[26] It is important to mention that peripheral astigmatism appears to be reduced with ICL implantation. This can be noted in the more rounded PSFs in **Figure 3D**. On the other hand, interestingly enough, the direction of the peripheral PSFs in the laser refractive surgery groups rotated for almost 90° after the surgical treatments. Zernike coefficients maps (**Figures D-K**) indicated that the rotation of the distortion was induced primarily by HOAs Z7 and Z8 because the two-dimensional pattern of these two parameters were reversed in the vertical (Z7) or horizontal (Z8) direction. Different from the laser refractive surgery groups, the peripheral PSF after the ICL implantation remained in the same direction as prior to the surgery, although it became rounder due to the elevated peripheral defocus. Another surprising finding was that most of the two-dimensional aberration patterns became flatter after the surgery (Z3, Z5, Z6, Z7, Z8, and Z12). However, we saw an asymmetric amount of remaining defocus in the horizontal direction (more hyperopia in temporal retina). It is speculated that the incision of ICL surgery was always made in the temporal side of the cornea in the study.

There was no statistical difference of the Strehl ratio values across the retina among the four groups. Although peripheral visual acuity was not measured in the current study, our clinical records showed that all patients achieved central visual acuity of better than 20/20 by the 3-month follow-up visit. Because the visual acuity is significantly lower in the periphery than in the fovea,[17-20] it is reasonable to expect that the different laser-based types of refractive surgeries would not produce a perceivable difference in peripheral visual acuity in real life.

The current study had several strengths. First, we used a high-resolution peripheral wavefront sensor to measure the two-dimensional peripheral optical quality of eyes prior to and after the refractive surgery. Second, four types of refractive surgeries were included for analysis, which covered the current main types of surgical treatments for myopia. However, it should be noted that the measurement was conducted without mydriasis in the current study. This would have limited the investigation of HOAs in a larger pupil. Second, the optical parameters of some visual complaints only perceived in a dim environment might not be completely detected by our instrument in the current mesopic conditions. Therefore, this might limit the ability for our findings to explain the correlation between visual symptoms and objective parameters.

FS-LASIK, Q-LASIK, SMILE, and ICL implantation produced a similarly satisfactory correction of refractive error and other objective optics quality metrics in the central retina. With regard to the peripheral retina, however, residual refractive error and relatively prominent PSF distortion was observed in ICL implantation. The different performance of these refractive surgeries in the peripheral retina deserves our notice and further investigation, because refractive surgeries have gained increasing popularity in young adults with myopia.

AUTHOR CONTRIBUTIONS

Study concept and design (ZL, YL, ZY, WL); data collection (ZL, YL); analysis and interpretation of data (ZL, PA, WL); writing the manuscript (ZL, YL); critical revision of the manuscript (ZL, PA, ZY, WL); statistical expertise (ZL); administrative, technical, or material support (ZL, YL, WL); supervision (PA, ZY, WL)

REFERENCES

1. Yang E, Roberts CJ, Mehta JS. A review of corneal biomechanics after LASIK and SMILE and the current methods of corneal biomechanical analysis. *J Clin Exp Ophthalmol*. 2015;6:1-6.
2. Zheng Y, Zhou YH, Zhang J, et al. Comparison of visual outcomes after femtosecond LASIK, wave front-guided femtosecond LASIK, and femtosecond lenticule extraction. *Cornea*. 2016;35(8):1057-1061. https://doi.org/10.1097/ICO.0000000000000891 PMID:27348719
3. Kim TI, Alió Del Barrio JL, Wilkins M, Cochener B, Ang M. Refractive surgery. *Lancet*. 2019;393(10185):2085-2098. https://doi.org/10.1016/S0140-6736(18)33209-4 PMID:31106754
4. Chen X, Guo L, Han T, Wu L, Wang X, Zhou X. Contralateral eye comparison of the long-term visual quality and stability between implantable collamer lens and laser refractive surgery for myopia. *Acta Ophthalmol*. 2019;97(3):e471-e478. https://doi.org/10.1111/aos.13846 PMID:30187653
5. Artal P, Derrington AM, Colombo E. Refraction, aliasing, and the absence of motion reversals in peripheral vision. *Vision Res*. 1995;35(7):939-947. https://doi.org/10.1016/0042-6989(94)00180-T PMID:7762151
6. Wang YZ, Thibos LN, Bradley A. Effects of refractive error on detection acuity and resolution acuity in peripheral vision. *Invest Ophthalmol Vis Sci*. 1997;38(10):2134-2143. PMID:9331277
7. Schallhorn SC, Venter JA, Hannan SJ, Hettinger KA, Teenan D. Effect of postoperative keratometry on quality of vision in the postoperative period after myopic wavefront-guided laser in situ keratomileusis. *J Cataract Refract Surg*. 2015;41(12):2715-2723. https://doi.org/10.1016/j.jcrs.2015.06.034 PMID:26796452
8. Hiatt JA, Grant CN, Wachler BS. Complex wavefront-guided retreatments with the Alcon CustomCornea platform after prior LASIK. *J Refract Surg*. 2006;22(1):48-53. https://doi.org/10.3928/1081-597X-20060101-11 PMID:16447936
9. Wang S, Lin Z, Xi X, et al. Two-dimensional, high-resolution peripheral refraction in adults with isomyopia and anisomyopia. *Invest Ophthalmol Vis Sci*. 2020;61(6):16-16. https://doi.org/10.1167/iovs.61.6.16 PMID:32511693
10. Lin Z, Duarte-Toledo R, Manzanera S, Lan W, Artal P, Yang Z. Two-dimensional peripheral refraction and retinal image quality in orthokeratology lens wearers. *Biomed Opt Express*. 2020;11(7):3523-3533. https://doi.org/10.1364/BOE.397077 PMID:33014548
11. Lan W, Lin Z, Yang Z, Artal P. Two-dimensional peripheral refraction and retinal image quality in emmetropic children. *Sci Rep*. 2019;9(1):16203. https://doi.org/10.1038/s41598-019-52533-7 PMID:31700132
12. Chen X, Miao H, Naidu RK, Wang X, Zhou X. Comparison of early changes in and factors affecting vault following posterior chamber phakic Implantable Collamer Lens implantation without and with a central hole (ICL V4 and ICL V4c). *BMC Ophthalmol*. 2016;16(1):161. https://doi.org/10.1186/s12886-016-0336-8 PMID:27604229
13. Jaeken B, Lundström L, Artal P. Fast scanning peripheral wavefront sensor for the human eye. *Opt Express*. 2011;19(8):7903-7913. https://doi.org/10.1364/OE.19.007903 PMID:21503102
14. Jaeken B, Tabernero J, Schaeffel F, Artal P. Comparison of two scanning instruments to measure peripheral refraction in the human eye. *J Opt Soc Am A Opt Image Sci Vis*. 2012;29(3):258-264. https://doi.org/10.1364/JOSAA.29.000258 PMID:22472755
15. Dorronsoro C, Remon L, Merayo-Lloves J, Marcos S. Experimental evaluation of optimized ablation patterns for laser refractive surgery. *Opt Express*. 2009;17(17):15292-15307. https://doi.org/10.1364/OE.17.015292 PMID:19688008
16. Kwon Y, Choi M, Bott S. Impact of ablation efficiency reduction on post-surgery corneal asphericity: simulation of the laser refractive surgery with a flying spot laser beam. *Opt Express*. 2008;16(16):11808-11821. https://doi.org/10.1364/OE.16.011808 PMID:18679453
17. Frisén L, Glansholm A. Optical and neural resolution in peripheral vision. *Invest Ophthalmol*. 1975;14(7):528-536. PMID:1140911
18. Wang YZ, Thibos LN, Bradley A. Effects of refractive error on detection acuity and resolution acuity in peripheral vision. *Invest Ophthalmol Vis Sci*. 1997;38(10):2134-2143. PMID:9331277
19. Anderson RS, Thibos LN. Relationship between acuity for gratings and for tumbling-E letters in peripheral vision. *J Opt Soc Am A Opt Image Sci Vis*. 1999;16(10):2321-2333. https://doi.org/10.1364/JOSAA.16.002321 PMID:10517018
20. Low FN. Peripheral visual acuity. *AMA Arch Opthalmol*. 1951;45(1):80-99. https://doi.org/10.1001/archopht.1951.01700010083011 PMID:14789295
21. Schumacher N, Schmidt M, Reer R, Braumann KM. Peripheral vision tests in sports: training effects and reliability of peripheral perception test. *Int J Environ Res Public Health*. 2019;16(24):E5001. https://doi.org/10.3390/ijerph16245001 PMID:31835309
22. Klostermann A, Vater C, Kredel R, Hossner EJ. Perception and action in sports: on the functionality of foveal and peripheral vision. *Front Sports Act Living*. 2019;1:66.
23. Wolfe B, Dobres J, Rosenholtz R, Reimer B. More than the useful field: considering peripheral vision in driving. *Appl Ergon*. 2017;65(316-325. https://doi.org/10.1016/j.apergo.2017.07.009
24. Artal P, Ginis H, Christaras D, Villegas EA, Prieto P. An intraocular lens to improve field curvature and off-axis astigmatism in pseudophakic patients. *Invest Ophthalmol Vis Sci*. 2020;61(7):848-848.
25. Zhang Y, Chen H, Zhang Y, Yang Y. The differences of corneal astigmatism in different populations and its quantitative analysis. *Afr Health Sci*. 2020;20(2):775-778. https://doi.org/10.4314/ahs.v20i2.30 PMID:33163043
26. Villegas EA, Marín JM, Ginis H, et al. Peripheral refraction and contrast detection sensitivity in pseudophakic patients implanted with a new meniscus intraocular lens. *J Refract Surg*. 2022;38(4):229-234. https://doi.org/10.3928/1081597X-20220113-01 PMID:35412927

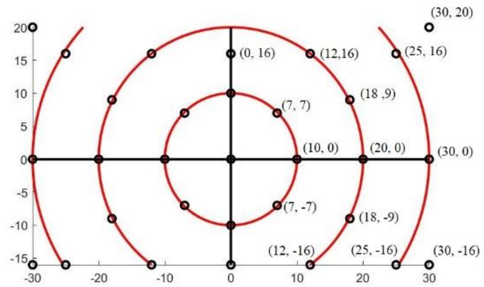

Figure A. The points selected to produce the point spread function images for the peripheral visual field. The radius of the circles are 10°, 20°, and 30° from inner to outer circle, respectively. The coordinates of the points in the right-half of the figure are labeled to better demonstrate the position.

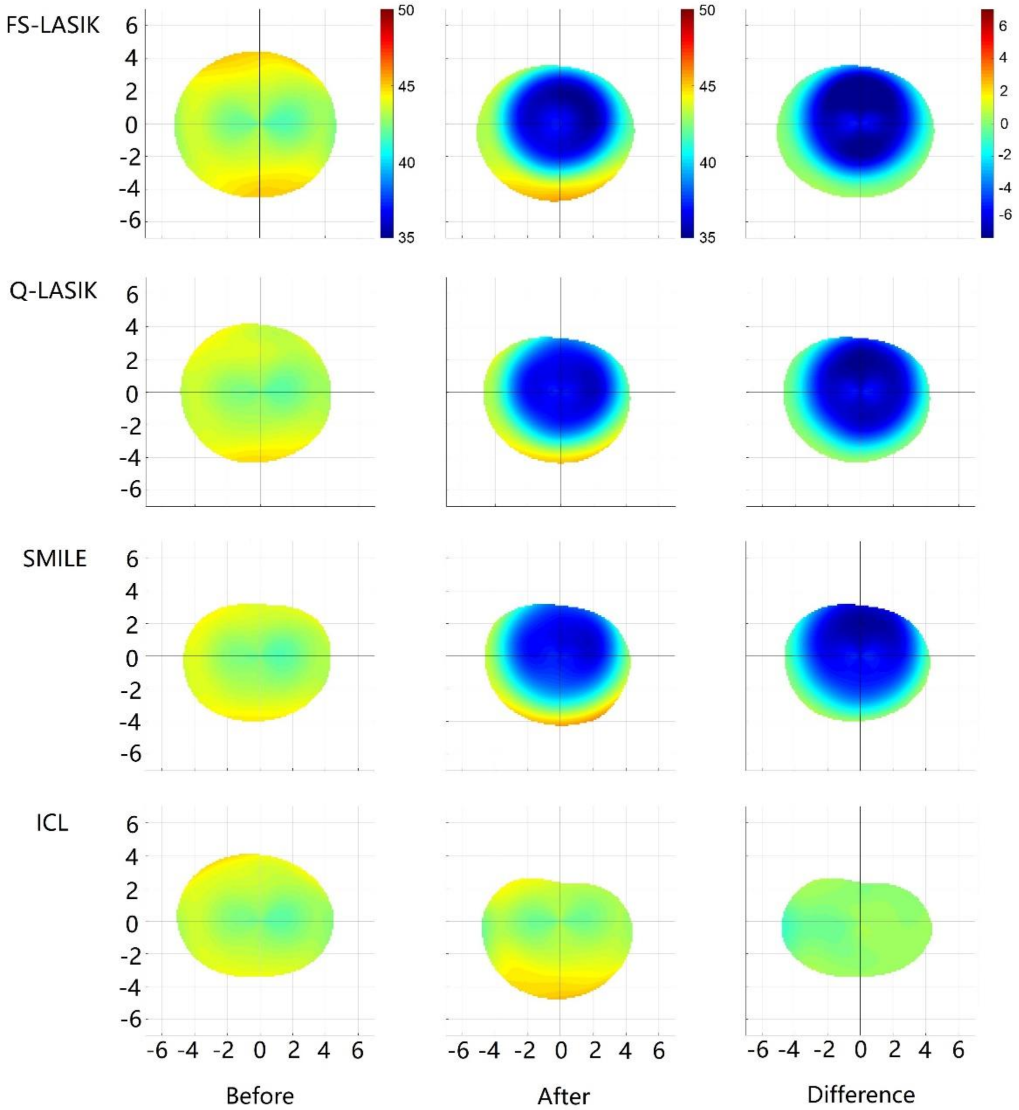

Figure B. Averaged total corneal power map. Left column: preoperative map. Middle column: postoperative map. Right column: change (after–before). The power maps are the averaged matrix of volunteers from the femtosecond laser–assisted laser in situ keratomileusis (FS-LASIK), Q-value guided customized laser in situ keratomileusis (Q-LASIK), small incision lenticule extraction (SMILE), and Implantable Collamer Lens (ICL) (STAAR Surgical) implantation groups. The units are in millimeters in coordinates. The color code is in diopters.

Table A
Aberrations in Central Retina (FS-LASIK Group)[a]

Zernike Polynomial (4 mm)	**Preoperative**	**Postoperative**	**tstat**	***P*[b]**
Z3	0.072 ± 0.141	-0.016 ± 0.086	1.85	.094
Z4[c,d]	4.362 ± 0.772	0.295 ± 0.134	16.93	< .001
Z5[d]	-0.595 ± 0.308	0.112 ± 0.265	-5.38	< .001
Z6[c,d]	0.025 ± 0.065	0.012 ± 0.072	0.669	.519
Z7[d]	-0.008 ± 0.067	-0.042 ± 0.07	1.247	.24
Z8	-0.008 ± 0.05	-0.021 ± 0.085	0.454	.66
Z9[d]	-0.015 ± 0.058	0.054 ± 0.082	-2.27	.046
Z12[d]	0.007 ± 0.039	0 ± 0.026	0.73	.482
3rd-order RMS	0.112 ± 0.043	0.138 ± 0.093	-1.224	.249
4th-order RMS	0.065 ± 0.022	0.085 ± 0.086	-0.775	.456
5th-order RMS	0.038 ± 0.022	0.068 ± 0.068	-1.646	.13
RMS HOAs[c]	0.153 ± 0.037	0.214 ± 0.193	-1.213	.253

FS-LASIK = femtosecond laser–assisted laser in situ keratomileusis; HOAs = higher order aberrations; RMS = root mean square of all aberrations in corresponding order

[a]Zernike coefficients in 4-mm pupil. Aberrations were expressed as mean ± standard deviation. Lower order aberrations: Z3 (oblique astigmatism), Z4 (defocus), and Z5 (with-the-rule/against-the-rule astigmatism). HOAs: Z6 (oblique trefoil, 3rd-order), Z7 (vertical coma, 3rd-order), Z8 (horizontal coma, 3rd-order), Z9 (horizontal trefoil, 3rd-order), and Z12 (spherical aberration, 5th-order).

[b]Comparison between preoperatively and postoperatively.

[c]Significant difference exists among four types of surgeries in preoperative condition.

[d]Significant difference exists among four types of surgeries in postoperative condition.

Table B
Aberrations in Central Retina (Q-LASIK Group)[a]

Zernike Polynomial (4 mm)	Preoperative	Postoperative	tstat	*P*[b]
Z3	-0.004 ± 0.186	0.029 ± 0.131	-0.78	.444
Z4[c,d]	4.577 ± 0.659	0.462 ± 0.194	30.619	< .001
Z5[d]	-0.36 ± 0.364	0.026 ± 0.141	-5.044	< .001
Z6[c,d]	-0.04 ± 0.072	-0.026 ± 0.051	-1.186	.25
Z7[d]	0.036 ± 0.111	0 ± 0.08	1.208	.241
Z8	-0.007 ± 0.068	-0.011 ± 0.053	0.283	.78
Z9[d]	0 ± 0.061	0.006 ± 0.058	-0.459	.651
Z12[d]	0.045 ± 0.057	0.028 ± 0.04	1.681	.108
3rd-order RMS	0.154 ± 0.068	0.115 ± 0.045	2.356	.029
4th-order RMS	0.09 ± 0.04	0.077 ± 0.032	1.15	.264
5th-order RMS	0.047 ± 0.027	0.037 ± 0.013	1.4	.177
RMS HOAs[c]	0.22 ± 0.073	0.159 ± 0.047	3.257	.004

HOAs = higher order aberrations; Q-LASIK = Q-value guided customized laser in situ keratomileusis; RMS = root mean square of all aberrations in corresponding order

[a]Zernike coefficients in 4-mm pupil. Aberrations were expressed as mean ± standard deviation. Lower order aberrations: Z3 (oblique astigmatism), Z4 (defocus), and Z5 (with-the-rule/against-the-rule astigmatism). HOAs: Z6 (oblique trefoil, 3rd-order), Z7 (vertical coma, 3rd-order), Z8 (horizontal coma, 3rd-order), Z9 (horizontal trefoil, 3rd-order), and Z12 (spherical aberration, 5th-order).

[b]Comparison between preoperatively and postoperatively.

[c]Significant difference exists among four types of surgeries in preoperative condition.

[d]Significant difference exists among four types of surgeries in postoperative condition.

Table C
Aberrations in Central Retina (SMILE Group)[a]

Zernike Polynomial (4 mm)	Preoperative	Postoperative	tstat	*P*[b]
Z3	-0.026 ± 0.173	-0.04 ± 0.117	0.31	.761
Z4[c,d]	4.21 ± 0.651	0.453 ± 0.16	23.602	< .001
Z5[d]	-0.223 ± 0.296	-0.008 ± 0.175	-3.171	.007
Z6[c,d]	-0.02 ± 0.063	-0.002 ± 0.051	-1.038	.317
Z7[d]	0.041 ± 0.084	-0.056 ± 0.065	3.458	.004
Z8	0.018 ± 0.04	0.015 ± 0.04	0.252	.805
Z9[d]	0.024 ± 0.06	0.078 ± 0.055	-2.674	.018
Z12[d]	0.055 ± 0.043	0.046 ± 0.037	0.737	.473
3rd-order RMS	0.12 ± 0.064	0.131 ± 0.06	-0.56	.585
4th-order RMS	0.085 ± 0.033	0.089 ± 0.053	-0.267	.793
5th-order RMS	0.04 ± 0.02	0.052 ± 0.038	-1.081	.298
RMS HOAs[c]	0.182 ± 0.06	0.18 ± 0.074	0.033	.974

HOAs = higher order aberrations; RMS = root mean square of all aberrations in corresponding order; SMILE = small incision lenticule extraction

[a]Zernike coefficients in 4-mm pupil. Aberrations were expressed as mean ± standard deviation. Lower order aberrations: Z3 (oblique astigmatism), Z4 (defocus), and Z5 (with-the-rule/against-the-rule astigmatism). HOAs: Z6 (oblique trefoil, 3rd-order), Z7 (vertical coma, 3rd-order), Z8 (horizontal coma, 3rd-order), Z9 (horizontal trefoil, 3rd-order), and Z12 (spherical aberration, 5th-order).

[b]Comparison between preoperatively and postoperatively.

[c]Significant difference exists among four types of surgeries in preoperative condition.

[d]Significant difference exists among four types of surgeries in postoperative condition.

Table D

Aberrations in Central Retina (ICL Group)[a]

Zernike Polynomial (4 mm)	**Preoperative**	**Postoperative**	**tstat**	***P*[b]**
Z3	-0.011 ± 0.2	0.049 ± 0.129	-1.187	.259
Z4[c,d]	5.144 ± 0.7	0.314 ± 0.216	24.617	< .001
Z5[d]	-0.29 ± 0.282	-0.229 ± 0.182	-1.451	.173
Z6[c,d]	-0.027 ± 0.055	-0.064 ± 0.064	2.203	.048
Z7[d]	0.007 ± 0.07	0.025 ± 0.05	-1.276	.226
Z8	-0.02 ± 0.029	0.011 ± 0.033	-2.778	.017
Z9[d]	0.023 ± 0.062	0.041 ± 0.037	-1.317	.212
Z12[d]	0.037 ± 0.053	0.03 ± 0.039	0.569	.58
3rd-order RMS	0.109 ± 0.04	0.111 ± 0.054	-0.143	.889
4th-order RMS	0.08 ± 0.033	0.063 ± 0.046	1.44	.175
5th-order RMS	0.041 ± 0.019	0.044 ± 0.026	-0.366	.721
RMS HOAs[c]	0.163 ± 0.039	0.168 ± 0.067	-0.275	.79

HOAs = higher order aberrations; ICL = Implantable Collamer Lens (STAAR Surgical) implantation; RMS = root mean square of all aberrations in corresponding order

[a]Zernike coefficients in 4-mm pupil. Aberrations were expressed as mean ± standard deviation. Lower order aberrations: Z3 (oblique astigmatism), Z4 (defocus), and Z5 (with-the-rule/against-the-rule astigmatism). Higher-order aberrations: Z6 (oblique trefoil, 3rd-order), Z7 (vertical coma, 3rd-order), Z8 (horizontal coma, 3rd-order), Z9 (horizontal trefoil, 3rd-order), and Z12 (spherical aberration, 5th-order).

[b]Comparison between preoperatively and postoperatively.

[c]Significant difference exists among four types of surgeries in preoperative condition.

[d]Significant difference exists among four types of surgeries in postoperative condition.

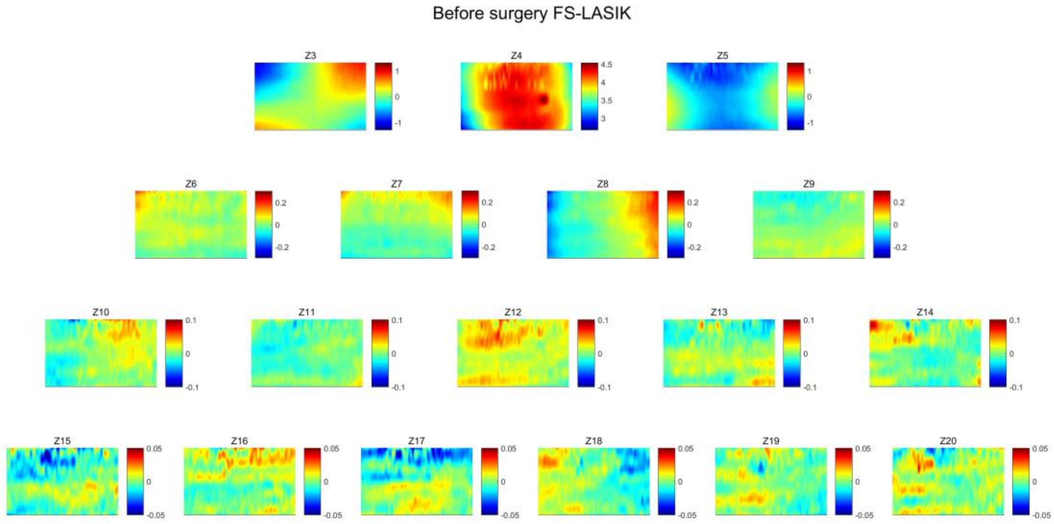

Figure C. The averaged Zernike coefficients maps from Z3 to Z20 for the femtosecond laser–assisted laser in situ keratomileusis (FS-LASIK) group prior to the surgery.

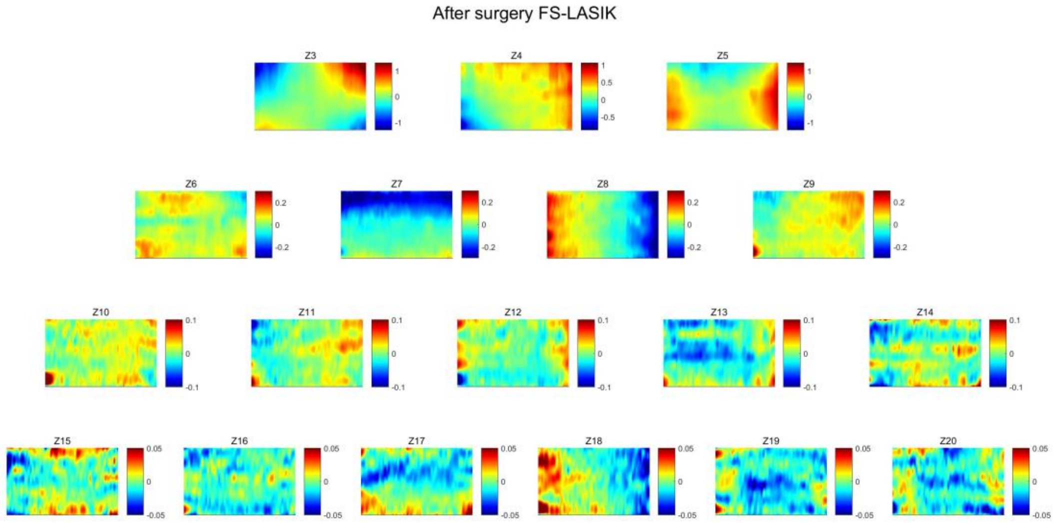

Figure D. The averaged Zernike coefficients maps from Z3 to Z20 for the femtosecond laser–assisted laser in situ keratomileusis (FS-LASIK) group after the surgery.

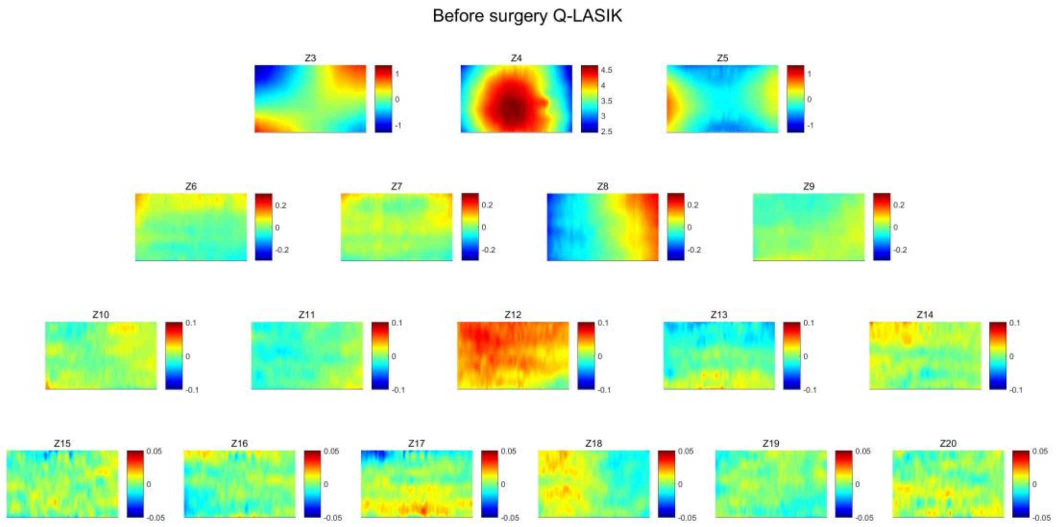

Figure E. The averaged Zernike coefficients maps from Z3 to Z20 for the Q-value guided customized laser in situ keratomileusis (Q-LASIK) group prior to the surgery.

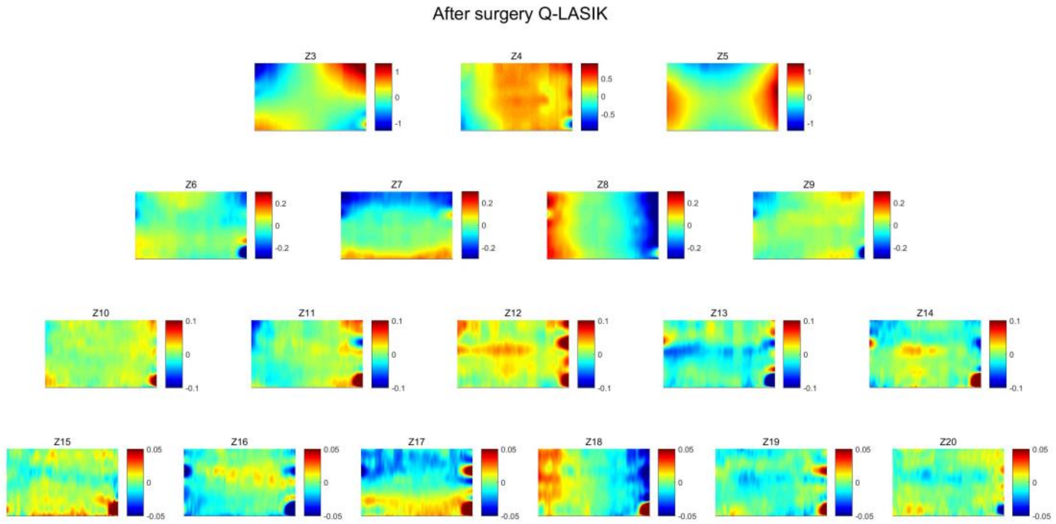

Figure F. The averaged Zernike coefficients maps from Z3 to Z20 for the Q-value guided customized laser in situ keratomileusis (Q-LASIK) group after the surgery.

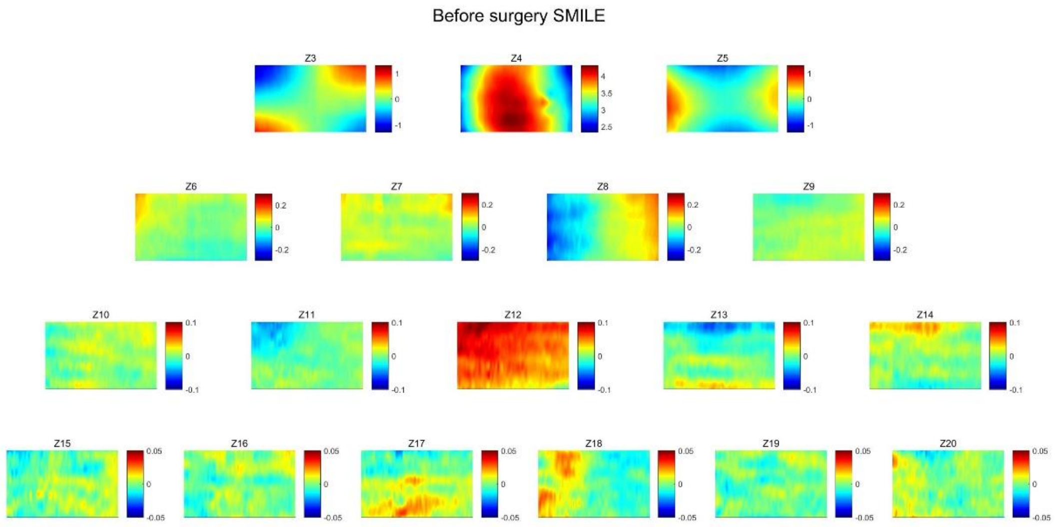

Figure G. The averaged Zernike coefficients maps from Z3 to Z20 for the small incision lenticule extraction (SMILE) group prior to the surgery.

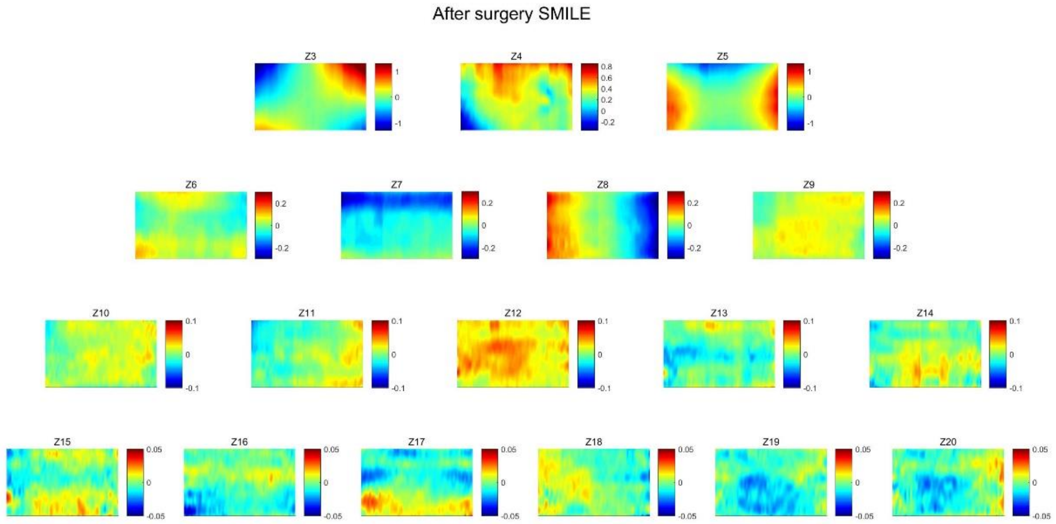

Figure H. The averaged Zernike coefficients maps from Z3 to Z20 for the small incision lenticule extraction (SMILE) group after the surgery.

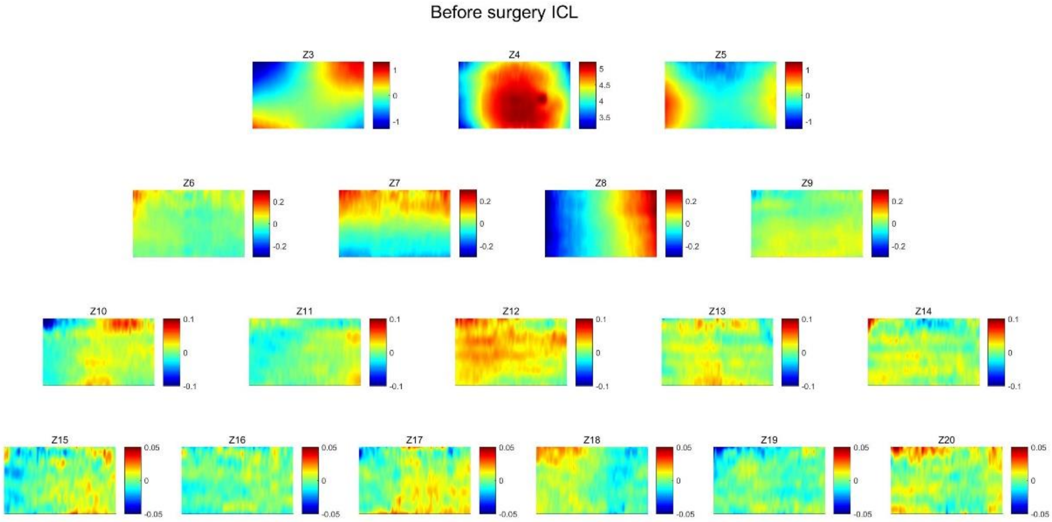

Figure I. The averaged Zernike coefficients maps from Z3 to Z20 for the Implantable Collamer Lens (ICL) (STAAR Surgical) implantation group prior to the surgery.

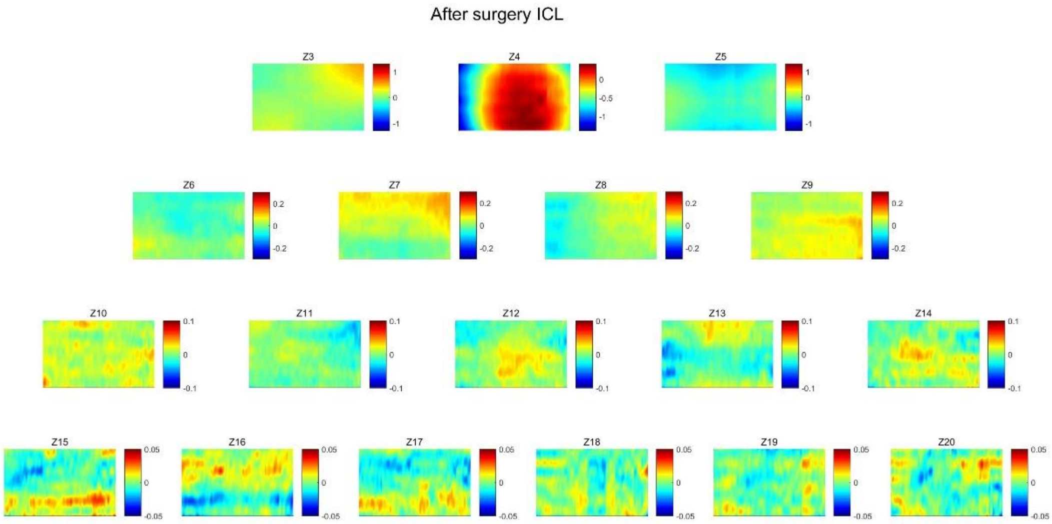

Figure J. The averaged Zernike coefficients maps from Z3 to Z20 for the small incision lenticule extraction (SMILE) group after the surgery.

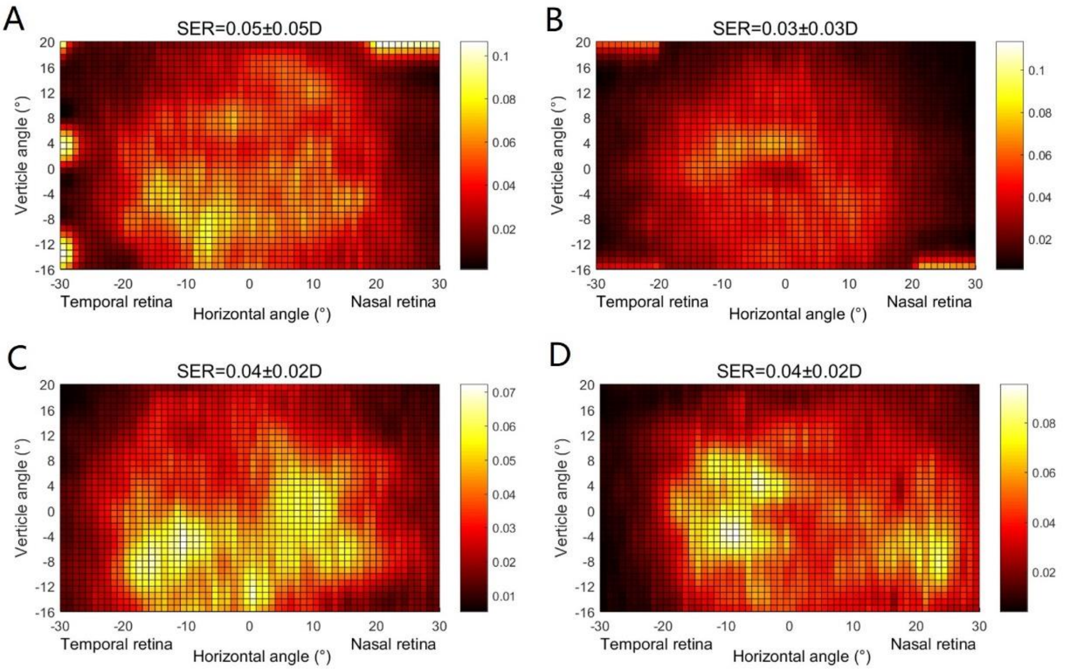

Figure K. The averaged Strehl ratio map: (A) femtosecond laser–assisted laser in situ keratomileusis (FS-LASIK), (B) Q-value guided customized laser in situ keratomileusis (Q-LASIK), (C) small incision lenticule extraction (SMILE), and (D) implantable Collamer Lens (ICL) (STAAR Surgical) implantation group. The brighter area indicates better image quality. No statistical difference was found in any region among the four groups. D = diopters; SER = spherical equivalent refraction

Table E
Average Strehl Ratio After Surgery in Each Region

Range	FS-LASIK Me (Q1-Q3) [Min, Max]	Q-LASIK Me (Q1-Q3) [Min, Max]	SMILE Me (Q1-Q3) [Min, Max]	ICL Me (Q1-Q3) [Min, Max]	*P*[a]
CEN	0.036 (0.023-0.063) [0.015, 0.173]	0.029 (0.014-0.044) [0.003, 0.125]	0.029 (0.015-0.059) [0.006, 0.078]	0.04 (0.029-0.043) [0.01, 0.067]	.414
R-8	0.051 (0.033-0.066) [0.02, 0.126]	0.052 (0.026-0.07) [0.006, 0.114]	0.045 (0.025-0.06) [0.012, 0.085]	0.048 (0.03-0.065) [0.02, 0.141]	.851
R-16	0.058 (0.035-0.071) [0.022, 0.091]	0.048 (0.036-0.065) [0.006, 0.081]	0.045 (0.034-0.052) [0.023, 0.074]	0.05 (0.04-0.063) [0.024, 0.102]	.721
R-20	0.058 (0.033-0.066) [0.021, 0.088]	0.045 (0.033-0.055) [0.009, 0.069]	0.04 (0.034-0.047) [0.024, 0.068]	0.043(0.035-0.061) [0.025, 0.085]	.596
R-25	0.05 (0.029-0.057) [0.02, 0.078]	0.039 (0.031-0.047) [0.014, 0.059]	0.037 (0.031-0.039) [0.022, 0.059]	0.041 (0.033-0.055) [0.026, 0.072]	.539
R-8-16	0.06 (0.035-0.071) [0.022, 0.1]	0.046 (0.034-0.064) [0.006, 0.076]	0.046 (0.037-0.048) [0.024, 0.07]	0.046 (0.036-0.066) [0.026, 0.09]	.809
R-16-20	0.038 (0.03-0.06) [0.019, 0.083]	0.034 (0.026-0.043) [0.014, 0.059]	0.033 (0.028, 0.04) [0.023, 0.067]	0.036 (0.029-0.051) [0.02, 0.066]	.553
R-20-25	0.024 (0.018-0.044) [0.015, 0.051]	0.025 (0.017-0.029) [0.009, 0.039]	0.026 (0.018-0.033) [0.013, 0.071]	0.03 (0.025-0.04) [0.018, 0.056]	.179

CEN = mean Strehl ratio in central retina; FS-LASIK = femtosecond laser–assisted laser in situ keratomileusis; ICL = Implantable Collamer Lens (STAAR Surgical) implantation; Q-LASIK = Q-value guided customized laser in situ keratomileusis; R-value: mean Strehl ratio within corresponding radius of circular region; R = radius 1 – radius 2: mean Strehl ratio within an annulus between the circulars within radius 1 and radius 2 (in degrees); SMILE = small incision lenticule extraction

[a]Kruskal-Wallis test.